Multiphoton Electron Angular Distributions from Laser-Aligned CS_2 Molecules

Vinod Kumarappan,[1,*] Lotte Holmegaard,[1] Christian Martiny,[2] Christian B. Madsen,[2] Thomas K. Kjeldsen,[2] Simon S. Viftrup,[1] Lars Bojer Madsen,[2,†] and Henrik Stapelfeldt[1,3,‡]

[1]*Department of Chemistry, University of Aarhus, 8000 Aarhus C, Denmark*

[2]*Lundbeck Foundation Theoretical Center for Quantum System Research, Department of Physics and Astronomy, University of Aarhus, 8000 Aarhus C, Denmark*

[3]*Interdisciplinary Nanoscience Center (iNANO), University of Aarhus, DK-8000 Aarhus C, Denmark*

(Received 3 December 2007; published 7 March 2008)

Laser-aligned carbondisulfide (CS_2) molecules are singly ionized by multiphoton absorption from intense, linearly polarized 25 fs laser pulses. The angular distribution of the photoelectrons exhibits a significant dependence on the angle between the polarizations of the aligning and ionizing laser fields. The widely used strong-field approximation predicts angular distributions in qualitative agreement with the experimental data but fails at a quantitative level.

DOI: 10.1103/PhysRevLett.100.093006 PACS numbers: 33.80.Rv, 33.60.+q, 42.50.Hz

The interaction between intense femtosecond laser pulses and molecules has attracted widespread interest over the past few years, fueled, e.g., by exciting opportunities for imaging molecular structure on the natural spatial and temporal scales [1–3]. In this context single ionization by linearly polarized laser pulses stands out as a process of special relevance because it triggers other strong-field phenomena such as high-harmonic generation and double ionization. Understanding molecular ionization by intense near infrared femtosecond laser pulses has therefore become a central theme explored in a variety of studies (see [4] for a recent review).

In particular, recent advances in the ability to control alignment of gas phase molecules, by short nonionizing laser pulses [5], are opening new possibilities for detailed insight into strong-field ionization mechanisms. So far, measurements of ion yields have illustrated the dependence of the total ionization probability on the field-molecule orientation [6–9], although not necessarily in accordance with theoretical predictions [9]. Related calculations in the molecular strong-field approximation (SFA) [10,11] and with the molecular tunneling theory [12] have shown that the ionization probability [13] as well as the emission direction of the photoelectrons [14–16] depends strongly on the molecular alignment with respect to the polarization of the ionizing pulse. The purpose of the present work is to report the first experimental evidence of the dependence of the photoelectron angular distributions on the laser field-molecule orientation. We use field-free aligned CS_2 molecules ionized in the multiphoton absorption regime to illustrate the effect [17]. Our experimental results are accompanied by numerical calculations using SFA and present the first direct comparison of this widely used theory and photoelectron angular distributions.

The experimental methods were described previously [18,19]. Briefly, a pulsed molecular beam, formed by supersonically expanding a gas mixture of ~20 mbar CS_2 and 100 bar helium into vacuum [15], is crossed at 90° by two pulsed, 800 nm, focused laser beams: the first to align the internuclear axis and the second to ionize the CS_2 molecules (Fig. 1). The 0.5 ps (FWHM) alignment pulse has a peak intensity of 2.9×10^{12} W/cm^2 when focused to a spotsize of $\omega_0 = 51$ μm. No ionization of CS_2 is observed from this pulse. The 25 fs (FWHM) ionizing pulse is focused to a spotsize $\omega_0 = 27$ μm and has a peak intensity of 7.7×10^{13} W/cm^2. At this intensity CS_2 primarily undergoes single ionization and dissociated fragment ions contribute no more than ~4%–5% of the total ion signal. Both pulses are linearly polarized and their relative angle is controlled by rotating a half-wave plate in the alignment beam. The electrons (or ions) produced by the ionization pulse are detected by a velocity map imaging spectrometer and recorded with a CCD camera.

Initially, by measuring the rotational dynamics following the alignment pulse, we ensure that the CS_2 molecules are well-aligned at the moment when the short ionization pulse is sent. The alignment pulse creates a coherent superposition of rotational states, i.e., a rotational wave packet, in each molecule. As a result the spatial orientation of the internuclear axis with respect to the alignment pulse polarization becomes time dependent. The spatial orientation is measured by Coulomb exploding the molecules using 3×10^{14} W/cm^2, 25 fs pulses and recording the direction of the S^+ ions [19]. At each time after the alignment pulse, recorded in steps of 0.33 ps, we determine $\langle \cos^2\theta_{2d} \rangle$, where θ_{2d} is the angle between the alignment pulse polarization and the projection of the S^+ velocity on the detector plane. Using this relative measure for the degree of alignment we identify that the best degree of field-free alignment occurs ~76 ps after the alignment pulse, corresponding to the peak of the first half rotational revival. At this time $\langle \cos^2\theta_{2d} \rangle = 0.76$ compared to the value of 0.50 obtained when no alignment pulse is included. In the subsequent measurements the delay of the ionization pulse is fixed at 76 ps.

Next, we measure the projected 2D photoelectron angular distributions as a function of the angle between the polarization $\boldsymbol{\epsilon} = \hat{\boldsymbol{x}}$ of the ionization pulse and the polar-

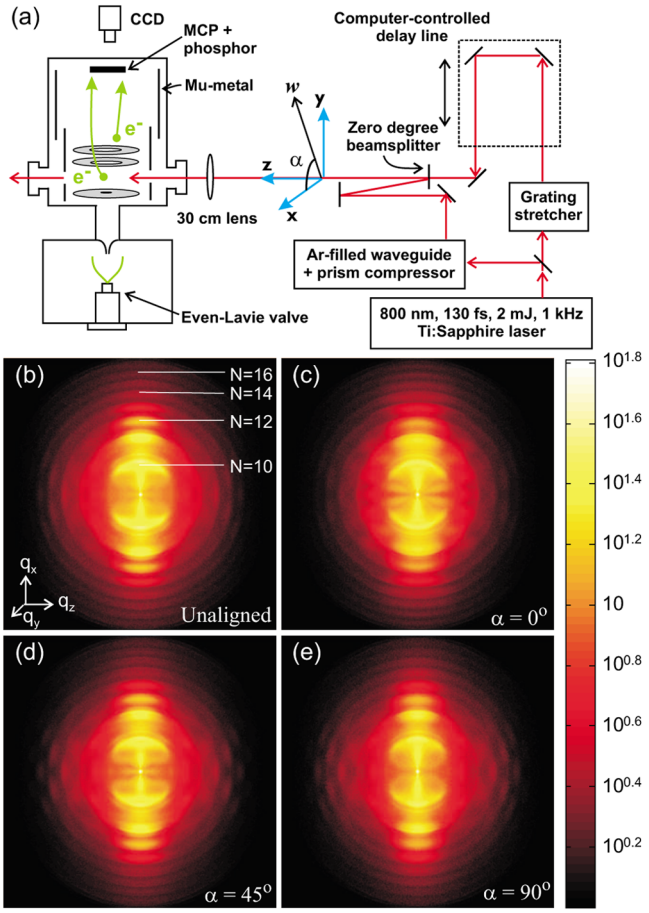

FIG. 1 (color online). (a) Schematic representation of the experimental setup, and laser propagation (along z) and polarization (along x) directions. The vector $\boldsymbol{w}$ represents the polarization of the alignment pulse, and hence the direction of alignment of the molecules. (b)–(e) 2D electron images as function of the vertical momentum q_x and the horizontal momentum q_z from multiphoton ionization of (b) unaligned molecules, and from aligned molecules with an angle (c) $\alpha = 0°$, (d) $\alpha = 45°$, (e) $\alpha = 90°$ between the polarizations of the alignment ($\boldsymbol{w}$) and ionizing ($\boldsymbol{\epsilon} = \hat{\boldsymbol{x}}$) pulse. The ring structure corresponds to different above-threshold ionization channels. In (b), N denotes the number of photon absorptions associated with the rings. The color scale is logarithmic.

ization $\boldsymbol{w}$ of the alignment pulse, i.e., the internuclear axis of CS_2. The coordinate system is detailed in Fig. 1(a). For all relative orientations the ionization pulse polarization was kept fixed, while the polarization of the alignment pulse was rotated. Electron images recorded at different relative orientations are displayed in Figs. 1(b)–1(e) as a function of the q_x (parallel with $\boldsymbol{\epsilon}$) and the q_z (perpendicular to $\boldsymbol{\epsilon}$) momenta, including a reference image (b) obtained with only the ionization pulse included.

Focusing first on the radial structure of the image it is seen that the momenta of the electrons and, therefore, their kinetic energies, are grouped around a series of discrete values, represented by the well-defined radial ring structure. This shows that ionization occurs in the multiphoton regime with the innermost pair of half rings corresponding to ionization by the minimum number of photons, 10, required to overcome the ionization threshold, $I_p = 10.08$ eV, at the peak intensity 7.7×10^{13} W/cm^2, of the ionization pulse [20]. Each of the subsequent pair of half rings in the progression at larger radii results from absorption of additional photons. Note that very sharp radial substructures in the two innermost pairs of half rings, corresponding to the lowest multiphoton orders, are observed. They are due to Rydberg states brought into resonance by the ac Stark shift [21].

Our interest here, however, is not the kinetic energy distributions of the electrons but rather their emission direction. In the four images displayed in Fig. 1 the bulk of the electron emission occurs along the polarization vector of the ionization pulse for all the multiphoton channels. There are, however, pronounced differences between the detailed electron emission patterns for different molecular orientations in Figs. 1(c)–1(e). These differences are particularly pronounced for electrons in the outermost rings emitted perpendicular to the polarization of the ionizing pulse, i.e., along the z axis in Fig. 1. This is clearly seen by comparing, for instance, the $N = 12$-, 13- and 14-photon channels recorded in the parallel geometry [Fig. 1(c)] and the perpendicular geometry [Fig. 1(e)].

To quantify the dependence of the electron emission on the relative orientation α we determined the photoelectron angular distribution (PAD) at the different α's for each individual multiphoton channel by integrating radially over the corresponding pair of half rings in the images. The results, represented as the number of electrons recorded per laser pulse versus ϕ_{2d} are displayed in Fig. 2, where ϕ_{2d} is the angle between the 2D projected electron ejection direction and the vertical ionizing pulse polarization. The angular resolution is better than 10 degrees. The PADs are

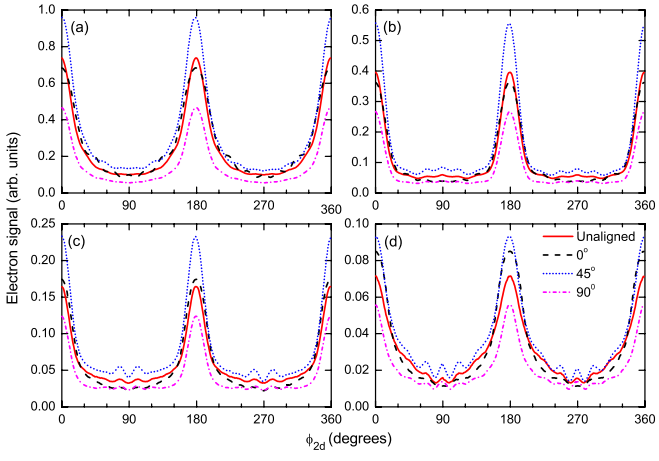

FIG. 2 (color online). Experimental PADs for the (a) 11-, (b) 12-, (c) 13-, and (d) 14-photon ionization channels extracted from Figs. 1(b)–1(e). The legend in (d) applies to all panels.

shown without an alignment pulse and at $\alpha = 0°, 45°$ and 90° for the (a) 11-, (b) 12-, (c) 13-, and (d) 14-photon channels.

First, we note that the magnitude of the electron signal depends on the orientation α. The $\alpha = 45°$ geometry provides the largest and the 90° geometry the smallest signals. This observation is consistent with recent measurements, based on detection of ion yields, on the orientational dependence of intense-laser single ionization of the CO_2 molecule [9], whose highest occupied molecular orbital (HOMO) has π_g symmetry as in CS_2. Second, the PADs change qualitatively between the different orientations for electrons centered around 90° or 270° (i.e., along the z axis). For example, in the 12-photon channel [Fig. 2(b)] there is a local maximum in the PAD at $\phi_{2d} = 90°$ for $\alpha = 45°$, whereas the PAD recorded for $\alpha = 0°$ exhibits a global minimum at $\phi_{2d} = 90°$. Similar differences between the angular distributions recorded at different orientations are observed for the 13-photon and 14-photon channels.

To model the experimental data, we calculate the 2D (q_x, q_z) momentum distribution $dP/dq_x dq_z(\mathbf{\Omega}_R)$ of an electron ejected from the HOMO of the CS_2 molecule oriented with its internuclear axis $\boldsymbol{R}$ in a solid angle $\mathbf{\Omega}_R$ with respect to the laboratory fixed coordinate system [see Fig. 1(a)]. The projected 2D momentum distribution is calculated from the probability amplitude for direct ionization $T_{fi}(\boldsymbol{q}, \mathbf{\Omega}_R)$ by $dP/dq_x dq_z(\mathbf{\Omega}_R) = \int_0^\infty |T_{fi}(\boldsymbol{q}, \mathbf{\Omega}_R)|^2 dq_y$. We obtain $T_{fi}(\boldsymbol{q}, \mathbf{\Omega}_R)$ in the length gauge molecular SFA [11] with a Volkov final state and as initial state the HOMO of CS_2 determined using GAMESS [22]. The evaluation of the T-matrix is performed by standard techniques detailed elsewhere [23,24]. All results include an averaging over the focal volume [25]. The theoretical prediction of the measured signal is then obtained by averaging the contributions from different orientations [26] $S(q_x, q_z, \alpha) = \int d\mathbf{\Omega}_R G_\alpha(\mathbf{\Omega}_R) dP/dq_x dq_z(\mathbf{\Omega}_R)$, where $G_\alpha(\mathbf{\Omega}_R)$ is the alignment distribution of the CS_2 molecules aligned along the direction given by the angle α (cf. Fig. 1). The formula for the rotational averaging is accurate in the present case where the molecules have no time to rotate during the ionizing fs pulse [26]. We obtain $G_\alpha(\mathbf{\Omega}_R)$ by the procedure described in [27] using a parallel (perpendicular) polarizability volume of 15.6 Å^3 (5.3 Å^3) and a linearly polarized aligning pulse with peak intensity 2.9×10^{12} W/cm^2 and duration of 500 fs (FWHM). The initial rotational temperature is taken to be 2 K. The ionizing pulse is fired 75.8 ps after the peak of the alignment pulse when maximal alignment is obtained (in excellent agreement with the experimental value, 76 ps). The theoretical alignment distribution has $\langle \cos^2 \theta_{2d} \rangle = 0.84$, and we have checked that our numerical results are essentially unaffected by changing to a broader alignment distribution that coincides with the experimental value $\langle \cos^2 \theta_{2d} \rangle = 0.76$.

Figure 3 shows results using the theoretical model. We concentrate on angular distributions corresponding to the 11-, 12-, 13- and 14-photon absorption channels of Figs. 2(a)–2(d). As in the experimental case, we localize the different ionization channels from the calculated 2D momentum distribution [20]. The results in the figure show a qualitative agreement with the experiment with minima at $\phi_{2d} = 90°$ (270°) and maxima around $\phi_{2d} = 0°$ (180°), but the detailed modulation differs somewhat in size and shape from the experimental observations. At a quantitative level, on the other hand, there are significant differences. In the experimental data there is typically a factor of 8 between the minimum and the maximum in each PAD, whereas in the theoretical result this factor is ~5.9–8.1 in the 11-, ~11.5–38.0 in the 12-, ~20.0–77.0 in the 13- and ~46.0–85.0 in the 14-photon absorption channel. Hence the theoretical model generally overestimates the ϕ_{2d} dependence. Turning to the magnitudes of the electron signals in Fig. 3, theory predicts in decreasing order $\alpha = 0°, 45°$, unaligned and 90°. In the experimental data, the order is 45°, unaligned, 0°, and 90° for the 11- and 12- photon absorption channels while it is 45°, 0°, unaligned, and 90° in the 13- and 14-photon absorption channels.

We have investigated several possible reasons for the discrepancy between the measurements and the predictions of the SFA. First, we found that there is no effect of ionization from the second highest occupied orbital, primarily because its binding energy of 14.60 eV leads to a strongly reduced ionization probability compared to that of the HOMO; $I_p = 10.08$ eV. Second, we found that there is no significant change in the ionization probability or in the

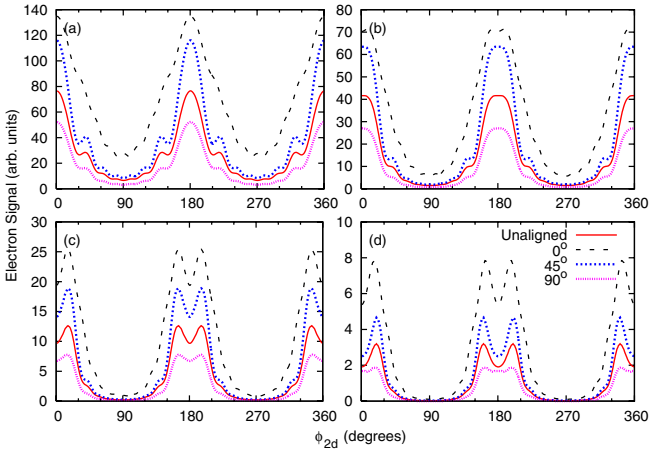

FIG. 3 (color online). Calculated PADs using laser pulse parameters identical to the experimental values. (a)–(d) represent the signals obtained by integrating the $dP/dq_x dq_z$ distribution over the circular areas identified as different ATI channels (see text). The different curves correspond to the unaligned, $\alpha = 0°$, $\alpha = 45°$, and $\alpha = 90°$ geometries as detailed by the legends in (d). For ease of comparison, we have scaled the $\alpha = 90°$ alignment by a factor of 3.

overall form of the PADs if the S-C-S angle is reduced from 180° to 140°. This rules out the influence from possible bending (due to electronic or vibrational excitation) during the ionization pulse. Rather, we believe that the discrepancy is associated with the excited state spectrum of the CS_2 molecule and possibly with the final state Coulomb interaction, none of which are accounted for in the SFA. In particular, recent strong-field multiphoton ionization studies of atoms have shown the crucial importance of high-lying Rydberg states, ac Stark shifted into resonance, for the detailed energy and angular distribution of photoelectrons [21]. The signatures of intermediate Rydberg resonances observed in our experimental data (Fig. 1) indicate a similar strong influence of excited states. Unlike atoms, however, no standard approach exists for calculating the excited electronic states of molecules even in a simple system like CS_2. Thus, we end by noting that the ability to align a molecular ensemble prior to the interaction with an intense femtosecond laser pulse presents new challenges for theory in the description of even the first ionization step.

In summary, we have presented the first experimental observations of orientationally resolved PADs using laser-aligned molecules. Many interesting improvements and applications of the present work can be envisioned. The orientational contrast of the PADs can be significantly increased by enhancing the degree of alignment using appropriately shaped laser pulses. Also, PADs from three-dimensionally aligned asymmetric top molecules [28,29] should be possible, thus generalizing the linear molecule, one-dimensional alignment case discussed here. Finally, (field-free) aligned molecules may be used for time-resolved studies of light-induced molecular changes, in particular, photodissociation [30].

This work is supported by the Carlsberg Foundation, the Lundbeck Foundation and the Danish Natural Science Research Council.

*Present address: Department of Physics, Kansas State University, Manhattan, Kansas 66506, USA.
†bojer@phys.au.dk
‡henriks@chem.au.dk

[1] J. Itatani, J. Levesque, D. Zeidler, H. Niikura, H. Pépin, J. C. Kieffer, P. B. Corkum, and D. M. Villeneuve, Nature (London) **432**, 867 (2004).
[2] S. Baker, J. Robinson, C. Haworth, H. Teng, R. Smith, C. Chirilă, M. Lein, J. Tisch, and J. Marangos, Science **312**, 424 (2006).
[3] N. Wagner, A. Wuest, I. Christov, T. Popmintchev, X. Zhou, M. Murnane, and H. Kapteyn, Proc. Natl. Acad. Sci. U.S.A. **103**, 13 279 (2006).
[4] M. Lein, J. Phys. B **40**, R135 (2007).
[5] H. Stapelfeldt and T. Seideman, Rev. Mod. Phys. **75**, 543 (2003).
[6] I. V. Litvinyuk, K. F. Lee, P. W. Dooley, D. M. Rayner, D. M. Villeneuve, and P. B. Corkum, Phys. Rev. Lett. **90**, 233003 (2003).
[7] A. S. Alnasser *et al.*, Phys. Rev. Lett. **93**, 113003 (2004).
[8] D. Pinkham and R. R. Jones, Phys. Rev. A **72**, 023418 (2005).
[9] D. Pavicic, K. F. Lee, D. M. Rayner, P. B. Corkum, and D. M. Villeneuve, Phys. Rev. Lett. **98**, 243001 (2007).
[10] J. Muth-Böhm, A. Becker, and F. H. M. Faisal, Phys. Rev. Lett. **85**, 2280 (2000).
[11] T. K. Kjeldsen and L. B. Madsen, J. Phys. B **37**, 2033 (2004).
[12] X. M. Tong, Z. X. Zhao, and C. D. Lin, Phys. Rev. A **66**, 033402 (2002).
[13] Z. X. Zhao, X. M. Tong, and C. D. Lin, Phys. Rev. A **67**, 043404 (2003).
[14] A. Jaroń-Becker, A. Becker, and F. H. M. Faisal, J. Phys. B **36**, L375 (2003).
[15] T. K. Kjeldsen, C. Z. Bisgaard, L. B. Madsen, and H. Stapelfeldt, Phys. Rev. A **68**, 063407 (2003).
[16] T. K. Kjeldsen, C. Z. Bisgaard, L. B. Madsen, and H. Stapelfeldt, Phys. Rev. A **71**, 013418 (2005).
[17] Related studies have been carried out on O_2, I. Litvinyuk *et al.* (unpublished).
[18] V. Kumarappan, C. Z. Bisgaard, S. S. Viftrup, L. Holmegaard, and H. Stapelfeldt, J. Chem. Phys. **125**, 194309 (2006).
[19] V. Kumarappan, S. S. Viftrup, L. Holmegaard, C. Bisgaard, and H. Stapelfeldt, Phys. Scr. **76**, C63 (2007).
[20] The kinetic energy of an electron ionized by N photons is $E_{\mathrm{kin}} = N\hbar\omega - U_p - I_p$, where the photon energy, $\hbar\omega$, is 1.55 eV and the ponderomotive energy, U_p, is 4.6 eV for the present peak intensity. A positive kinetic energy implies $N \geq 10$.
[21] R. Wiehle, B. Witzel, H. Helm, and E. Cormier, Phys. Rev. A **67**, 063405 (2003).
[22] M. W. Schmidt *et al.*, J. Comput. Chem. **14**, 1347 (1993).
[23] T. K. Kjeldsen and L. B. Madsen, Phys. Rev. A **74**, 023407 (2006).
[24] C. P. J. Martiny and L. B. Madsen, Phys. Rev. A **76**, 043416 (2007).
[25] Z. Chen, T. Morishita, A.-T. Le, and C. D. Lin, Phys. Rev. A **76**, 043402 (2007).
[26] C. B. Madsen, A. S. Mouritzen, T. K. Kjeldsen, and L. B. Madsen, Phys. Rev. A **76**, 035401 (2007).
[27] J. Ortigoso, M. Rodriguez, M. Gupta, and B. Friedrich, J. Chem. Phys. **110** 3870 (1999).
[28] J. J. Larsen, K. Hald, N. Bjerre, H. Stapelfeldt, and T. Seideman, Phys. Rev. Lett. **85**, 2470 (2000).
[29] K. F. Lee, D. M. Villeneuve, P. B. Corkum, A. Stolow, and J. G. Underwood, Phys. Rev. Lett. **97**, 173001 (2006).
[30] O. Geßner *et al.*, Science **311**, 219 (2006).